JOURNAL OF SPACECRAFT AND ROCKETS
Vol. 38, No. 6, November–December 2001

Transitional Flow over an Elliptic Cone at Mach 8

Xudong Xiao,* J. R. Edwards,† and H. A. Hassan‡
North Carolina State University, Raleigh, North Carolina 27695-7910

The k–ζ transitional/turbulence model is used to study the transitional flow over an elliptic cone of aspect ratio of 2:1 at Mach 8 and a range of Reynolds numbers. Although the configuration has been the subject of detailed experimental and computational investigations, it has not been possible to determine with certainty the instability mechanisms responsible for transition. The present analysis suggests that none of the obvious mechanisms, i.e., second-mode or crossflow, are responsible for the transition. Instead, a form of bypass transition resulting from large-amplitude disturbances appears to reproduce quite well the experimentally measured heat-transfer data and the onset and the extent of transition over a wide range of Reynolds numbers.

Nomenclature

b	=	model constant (second mode)
C_μ	=	constant, 0.09
c_1–c_5	=	model constants; Eqs. (13) and (15)
f	=	model constant (crossflow)
h	=	roughness height, ft
k	=	kinetic energy of fluctuation per mass, ft^2/s^2
M	=	Mach number
P	=	pressure, lb/ft^2
q_w	=	heat flux at wall, Btu/ft^2/s
Re	=	Reynolds number
S_{ij}	=	strain tensor
s	=	distance from vertex, ft
s_t	=	location of transition onset, ft
Tu	=	freestream fluctuation intensity
U_p	=	phase velocity, ft/s
u_i	=	mean velocity, ft/s
V_e	=	edge velocity, ft/s
β	=	parameter defined in Eqs. (18) and (19)
Γ	=	intermittency
δ	=	boundary-layer thickness, ft
δ^*	=	displacement thickness, ft
ζ	=	enstrophy, s^{-2}
λ	=	wavelength, ft
μ	=	viscosity, lb · s/ft^2
ν	=	kinematic viscosity, ft^2/s
ξ	=	parameter defined in Eq. (16)
ρ	=	density, slug/ft^3
τ	=	timescale, s
τ_{ij}	=	stress, lb/ft^2
τ_k	=	decay time, s
ω	=	frequency, s^{-1}

Subscripts

bp	=	bypass
cf	=	crossflow
e	=	boundary-layer edge
nt	=	nonturbulent
sm	=	second mode
t	=	turbulent

Received 2 February 2001; revision received 11 July 2001; accepted for publication 21 July 2001.

*Research Assistant, Mechanical and Aerospace Engineering.
†Associate Professor, Mechanical and Aerospace Engineering. Senior Member AIAA.
‡Professor, Mechanical and Aerospace Engineering. Associate Fellow AIAA.

Introduction

IT is generally believed that three instability mechanisms are responsible for transition over three-dimensional bodies in conventional hypersonic tunnels. These are second mode, crossflow, and a form of bypass transition[1] resulting from high disturbance environment (HIDE). Disturbances of such amplitude cannot be described by linear stability theory. In general, the bypass mechanism discussed by Mokovin[1] covers a class of transitional flows where the linear Tollmien–Schlichting (T–S) mechanism is completely bypassed by a nonlinear mechanism.[2]

To understand the role of such mechanisms, the flow over an elliptic cone of aspect ratio two and zero angle of attack at Mach number of eight was a subject of extensive investigation by Kimmel et al.[3] and Poggie et al.[4] The experiments were conducted at Tunnel B of the Arnold Engineering Development Center while computations were carried out using codes based on parabolized Navier–Stokes equations and e^n methods. Because of the complexity of the flow, the instability mechanisms were not identified. It was suggested, however, that a combination of traveling or stationary crossflow and second-mode instabilities might be the cause.

Because Tunnel B is characterized by freestream fluctuation intensities in excess of 1% (Ref. 5), the instability mechanisms suggested in Refs. 3 and 4 may not be the only ones responsible for transition. Further, because no single dominant instability mechanism was identified in the flow it is possible that resulting transition can be a result of nonlinear mode interactions. Thus interpretation based on linear stability theory might not be adequate.

Attention in this work is thus devoted to exploring the role of HIDE on transition in three-dimensional flows in conventional hypersonic facilities. The approach to be used is based on the k–ζ transitional/turbulence model. In this approach transitional flows are treated in a turbulencelike manner with the nonturbulent eddy viscosity deduced from the instability mechanism responsible for transition.[6,7] The theory in its present form is capable of treating both natural[6] and HIDE transitions.[7] The mechanism of natural transition can be derived from linear stability theory. This, however, is not the case for high-amplitude disturbances. As a result, dimensional considerations were used in Ref. 7 to deduce relevant timescales (or the frequency of the most amplified mode at a given location) for HIDE. This approach was demonstrated for transitional hypersonic flows in both quiet and conventional facilities for straight and flared cones at zero angle of attack.[8,9] Based on these investigations, it was found that transition was not a result of the growth of a single mode. Rather, when considering two-dimensional/axisymetric flows a linear combination of HIDE and second-mode mechanisms better reproduced experimental results in conventional hypersonic facilities, whereas a linear combination of the first oblique mode and second-mode better reproduced experimental results in quiet hypersonic facilities.

Calculations were carried out for the three candidate instability mechanisms: second-mode, crossflow, and HIDE. Because the surface pressure is approximately constant along rays emanating from the vertex, a criterion based on a minimum heat flux was employed to determine transition onset. Calculations are presented for four Reynolds numbers. Based on current and earlier calculations, it appears that transition in conventional hypersonic facilities is dominated by large-amplitude disturbances.

Formulation of the Problem

Approach

In the transitional/turbulence k–ζ model the eddy viscosity is set as

$$(1-\Gamma)\mu_{\rm nt} + \Gamma\mu_t$$

where $\mu_{\rm nt}$ is the eddy viscosity resulting from the nonturbulent fluctuations; $\mu_{\rm nt}$ is dependent on the instability mechanisms and can be written as

$$\mu_{\rm nt} = C_\mu \rho k \tau_{\rm nt}, \qquad C_\mu = 0.09 \tag{1}$$

where $\tau_{\rm nt}$ is the timescale of nonturbulent fluctuations. In general, $\tau_{\rm nt}$ is deduced from the frequency of the most amplified mode at a given location. In addition to modifying the eddy viscosity, the dissipation time scale in the k equation is chosen as

$$1/\tau_k = (1-\Gamma)/\tau_{k,\rm nt} + \Gamma/\tau_{k,t} \tag{2}$$

Expressions for $\tau_{\rm nt}$ and $\tau_{k,\rm nt}$ were developed[8,10] for crossflow and second-mode instabilities, whereas expressions appropriate for turbulent flow were taken from Ref. 11. The desired expressions for HIDE transition were developed[7] in terms of Re_s, where s is the distance along the surface in the mean flow direction. Such a formulation is not suited for three-dimensional applications and thus was rederived here in terms of Re_{δ^*}.

Expressions for the Various Timescales

Second-Mode Mechanism

At Mach numbers higher than approximating four, the transitional process for two-dimensional/axisymmetric flows without curvature is dominated by second-mode disturbances. Second-mode disturbances are acoustic disturbances characterized by large fluctuations in pressure and temperature that are much larger than velocity fluctuations. For this mode τ is chosen as

$$\tau_{\rm sm} = b/\omega_{\rm sm} \tag{3}$$

$$\omega_{\rm sm} = U_p/\lambda_{\rm sm} \tag{4}$$

U_p is about 0.94 of the edge velocity V_e, and $\lambda_{\rm sm}$ is approximately 2δ. In addition,

$$1/\tau_{k,\rm sm} = b(\mu_{\rm nt}/\mu)_{\rm sm} S \tag{5}$$

where

$$S^2 = S_{ij}S_{ij}, \qquad S_{ij} = \frac{1}{2}\left(\frac{\partial u_i}{\partial x_j} + \frac{\partial u_j}{\partial x_i}\right) \tag{6}$$

The value of b is chosen as 0.054. This value was arrived at in Ref. 8 from calculation of flows in a quiet tunnel at $M = 6$.

Crossflow Mechanism

The wavelength of the dominant crossflow disturbance varies with the boundary-layer thickness δ. In addition, crossflow instabilities are sensitive to surface roughness. It is shown in Ref. 10 that

$$\tau_{\rm cf} = f\lambda_{\rm cf}/V_e \tag{7}$$

where f depends on the surface roughness; $\lambda_{\rm cf}$ is in the range $3 \sim 4\delta$.

Müller and Bippes[12] demonstrated that the wavelengths of both traveling and stationary crossflow disturbances were the same but shifted in phase by $\lambda_{\rm cf}/2$. A value of $\lambda = 3.5\delta$ was adopted,[10] and this value will be employed here. The model constant f is a function of the surface finish and was correlated[10] as

$$f = 0.003\left[(h/h_{\rm ref})^{-0.8} Re_h - 0.92\right] \tag{8}$$

where

$$h_{\rm ref} = 1\ \mu m, \qquad Re_h = V_e h/\nu_e \tag{9}$$

and h is peak-to-peak distributed roughness level. For rms measured levels a sinusoidal distribution is assumed, and the level is increased by a factor of $\sqrt{2}$. For the present calculation h is assumed to be $0.81\sqrt{2}\ \mu$m (3.758×10^{-6} ft) (Ref. 13). The contribution of crossflow to the dissipation timescale is given by

$$1/\tau_{k,\rm cf} = f(\mu_{\rm nt}/\mu)_{\rm cf} S \tag{10}$$

The correlation indicated for f in Eq. (8) was arrived at from consideration of low-speed flows. It is not clear whether the same correlation will hold for high-speed flows. In spite of this, no adjustment of the model constant was made.

The timescales of second-mode and crossflow instabilities are proportional to δ/V_e. Thus, although one can distinguish these two types of instabilities from wavelength or frequency measurements $\tau_{\rm cf}$ and $\tau_{\rm sm}$ have essentially the same functional form, and, thus, predictions based on these two instabilities are somewhat similar:

$$\delta/V_e = \left(\nu/V_e^2\right)Re_\delta = \left(\nu/V_e^2\right)Re_{\delta^*}(\delta/\delta^*) \tag{11}$$

HIDE Mechanism

The timescales for the HIDE mechanism were derived in Ref. 7 and were used in Ref. 9 without any adjustment to study transitional axisymmetric flows in conventional hypersonic facilities. Because of the desire to avoid calculating typical boundary-layer thicknesses, the correlations were developed in terms of Re_s, where s is the distance measured along rays emanating from the vertex. Such correlations are not suited for three-dimensional flows. Instead, we opted to develop correlations in terms of δ^*. The resulting expression for the time scale $\tau_{\rm bp}$ is

$$\tau_{\rm bp} = c_1\left(\nu/V_e^2\right)Re_{\delta^*}^{c_2} \tag{12}$$

In the configuration under consideration, $\partial p/\partial s \approx 0$ along rays emanating from the vertex. This observation made it possible to deduce c_2 from the results of Ref. 7. Because

$$\frac{\delta^*}{s} = \frac{Re_{\delta^*}}{Re_s} \sim Re_s^{-\frac{1}{2}}, \qquad \left(\frac{\partial p}{\partial s} \approx 0\right), \qquad Re_{\delta^*} \sim Re_s^{\frac{1}{2}}$$

and therefore

$$c_2 = 2 \times 0.9448 Tu^{\frac{1}{8}} \approx 2.0 \tag{13}$$

where Tu is the average freestream fluctuation intensity.[14] As indicated in Ref. 5, this quantity is a function of both the Reynolds and Mach numbers. Because such information is, in general, not readily available, the theory of Ref. 7 was based on an average value. The value of $Tu = 1.25$ was deduced from Ref. 5 and used in Ref. 9. Because we are dealing with the same facility and the same range of Reynolds and Mach numbers, we opted to use the same value used earlier. In general, different values of Tu will result in different values of c_2. The coefficient c_1 and the other constants indicated next were arrived at from using the results of Ref. 7 and one of the test cases that correspond to a body length Reynolds number $Re_L = 6.7 \times 10^6$. Equation (12) is different from Eq. (11). Thus, one would expect that the behavior of this mode of instability is different from the others.

The contribution of the HIDE mechanism to the dissipation timescale is given by

$$1/\tau_{k,\rm bp} = [c_3(\mu_{\rm nt}/\mu) + c_4\Gamma]S + c_5(k/\nu) \tag{14}$$

where

$$c_1 = 0.00004, \qquad c_3 = 0.00002, \qquad c_4 = 0.15, \qquad c_5 = 0.001 \tag{15}$$

Intermittency and Onset Prediction Criteria

The intermittency Γ employed here is taken from Ref. 9 and is a modification of Dhawan and Narasimha's expression[15] suited for hypersonic flows in noisy tunnels. The expression for Γ is

$$\Gamma(s) = 1 - \exp(-0.412\xi^2), \qquad \xi = \max(s - s_t, 0.0)/\beta \quad (16)$$

Letting

$$Re_{\beta_0} = 9.0 Re_{s_t}^{0.75} \quad (17)$$

then the high-intensity correction is given by

$$\beta = \begin{cases} \beta_0, & Tu \le 0.5 \\ \beta_0/2Tu, & Tu > 0.5 \end{cases} \quad (18)$$

and the Mach-number correction is given by

$$\beta = \begin{cases} \beta_0, & Me^2 \le 7 \\ \frac{5}{12}\{1 + [(\gamma - 1)/2]Me^2\}\beta_0, & Me^2 > 7 \end{cases} \quad (19)$$

where Me is the edge Mach number.

Because the surface pressure is almost constant along rays emanating from the vertex, the onset is based on a minimum heat flux criterion. Thus, s_t that appears in Eq. (16) is determined along each ray, as part of the solution, by the location where wall heat flux is minimum.

Numerical Method

The Navier–Stokes equations are formulated in a cell-vertex finite difference manner, with the inviscid components discretized using Edwards's low-diffusion flux-splitting scheme (LDFSS).[16] This hybrid flux-vector/flux-difference splitting method captures shock waves without any oscillations while resolving free shear and boundary layers accurately. The upwind scheme is extended to second-order accuracy using slope-limited variable extrapolation techniques. Viscous and diffusion terms are discretized using central differences. The governing equations are formulated in a fully implicit fashion and advanced toward a steady-state solution using a planar Gauss–Seidel iteration strategy.[17] In this approach each streamwise-normal plane is solved using generalized minimum residual Krylov subspace method (GMRES).[18]

An inviscid calculation is carried out first to determine edge conditions. The boundary-layer thickness is determined as the height normal to the surface at which the velocity is 99% of the edge velocity. The transitional solution is started from the laminar solution. Because a minimum heat-flux criterion is used to determine transition onset, initial iterations are run with an assumed transition onset. This procedure is carried out by selecting onset points at $\theta = 0$ and 90 deg locations and employing linear interpolation for the intermediate points. As long as the initial points are selected ahead of the actual transitional locations, the solution is independent of the initial guess. After some 70 iterations in this mode, the minimum heat-flux criterion is employed throughout. The planar Gauss–Seidel method provides reasonably rapid convergence with fewer than 300 iterations typically required to obtain a solution.

Results and Discussion

The present theory is compared with the experimental measurements carried out on an elliptic cone in Tunnel B at a Mach number M_∞ of 7.93 and a stagnation temperature T_0 of 1310.4R (728 K). Comparisons are limited to cold wall conditions with a wall-to-stagnation-temperature ratio, $T_w/T_0 = 0.42$. The broadband rms mass flux was in the range of 1.2 to 1.5%. This quantity, which is assumed in this work to represent the freestream fluctuation intensity, is a function of the unit Reynolds number and Mach number. As explained earlier, a value of 1.25 is used here. The experimental model was a sharp-nosed cone with an elliptical cross section of aspect ratio of 2:1 and length of 40 in. (1.016 m); see Fig. 1. The cone half-angle is 7 deg along the minor axis. When using a cylindrical coordinate system, $\theta = 0$ deg corresponds to the top centerline, or minor axis endpoint, while $\theta = 90$ deg corresponds to the leading edge or major axis endpoint. Pressure and heat transition gauges were placed on separate quadrants. The heat-transfer gauges consist of 4.8-mm-diam Schmidt–Boelter gauges. These gauges have an uncertainty of $\pm 10\%$ in two-dimensional flows with greater uncertainty (unspecified) in three-dimensional flows.

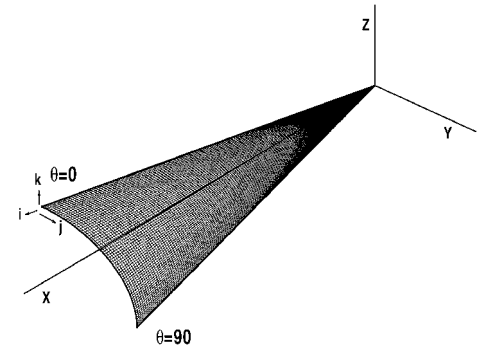

Fig. 1 Coordinate system.

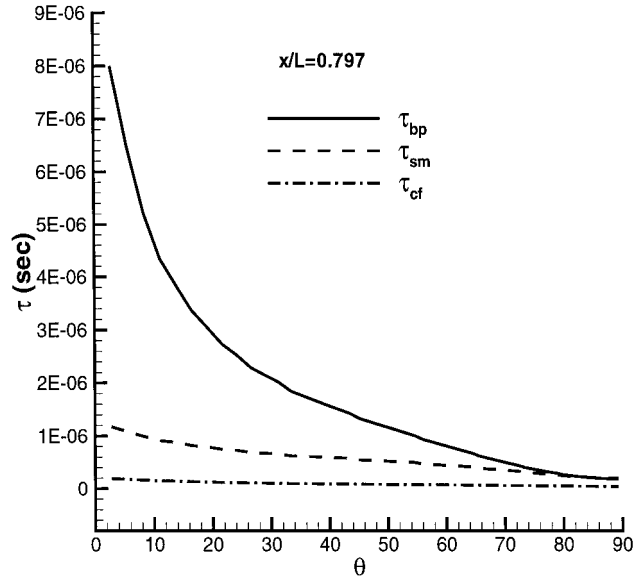

Fig. 2 Timescale circumferential distribution ($Re/L = 6.09 \times 10^5$/ft).

Figure 2 shows a comparison of timescales [see Eqs. (3), (7), and (12)] as a function of θ. These timescales are proportional to the inverse of respective frequencies with the proportionality model constants being dependent on environmental conditions. Thus, the inverse of the timescales is not equal to measured frequency of most amplified modes. The model constants are selected in such a way that the nonturbulent eddy viscosity should be comparable to the molecular shear viscosity before transition onset. The calculations also indicate that δ, V_e, and δ/V_e are maximum at $\theta = 0$ deg and minimum at $\theta = 90$ deg.

Comparison with experiment will be carried out for four unit Reynolds numbers (Re/L) of 6.09×10^5, 7.8×10^5, 1.03×10^6, and 1.98×10^6/ft. Grid-refinement studies were carried out for the highest unit Reynolds number. Three grids were considered for one-fourth of the cone, $129 \times 33 \times 73$, $129 \times 65 \times 73$, $195 \times 65 \times 73$ along mean flow, circumferential, and normal directions, respectively. The resolution in the normal direction was such that y^+ was less than 0.7 for all unit Reynolds numbers considered. All results presented here are for the $129 \times 65 \times 73$ grid.

Figure 3 shows a comparison between predicted and measured wall heat flux q_w at $\theta = 0$, 45, and 88 deg assuming a second-mode instability mechanism. As is seen from the figure, both the onset of transition and the magnitudes of the heat flux are poorly predicted. In an effort to explain the results, it is recalled that τ_{sm} scales like

$$\delta/V_e$$

The production of fluctuation kinetic energy in the nonturbulent region is

$$\tau_{ij}\frac{\partial u_i}{\partial x_j} \sim \tau_{\mathrm{nt}}\left(\frac{\partial u}{\partial y}\right)^2 \sim \frac{\delta}{V_e}\left(\frac{V_e}{\delta}\right)^2 \sim \frac{V_e}{\delta} \tag{20}$$

where τ_{ij} is the stress of the nonturbulent fluctuations. Now, V_e/δ is maximum at the shoulder. Thus, the model for this instability mechanism suggests that transition should take place first near the shoulder region and not at the top centerline. This is not in agreement with experiment. This somewhat qualitative argument may explain the observed behavior.

Because a similar scaling holds for the crossflow instability mechanism, similar results are obtained. The behavior indicated in Fig. 3 was typical of all other Reynolds numbers considered in this work. As a result, none of these results are shown here.

Figures 4–7 show a comparison of predicted and measured heat flux for four different unit Reynolds numbers at $\theta = 0$, 45, and 88 deg assuming a HIDE mechanism. As is seen from the figures, generally good agreement is indicated for onset prediction, extent, and heat flux. The only exception is peak heat transfer for $\theta = 88$ deg

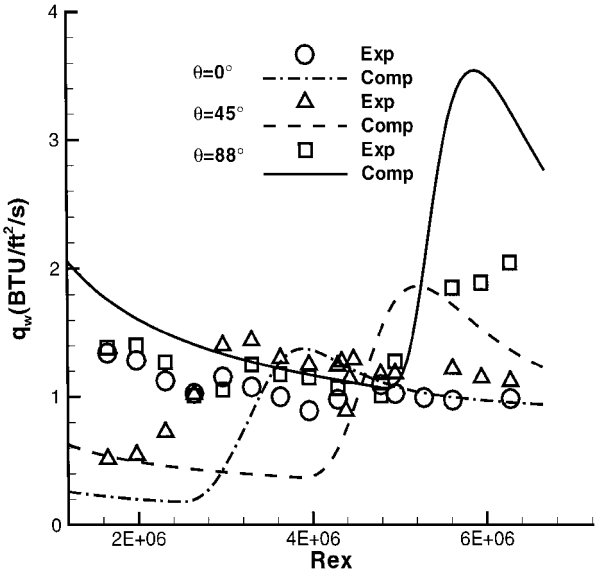

Fig. 3 Heat-flux distribution along the rays of cone (Re/L = 1.98 × 10^6/ft, second mode).

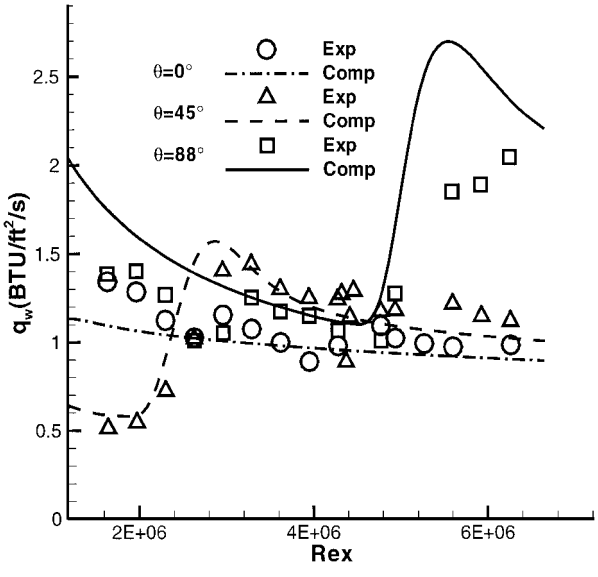

Fig. 4 Heat-flux distribution along the rays of cone (Re/L = 1.98 × 10^6/ft, HIDE).

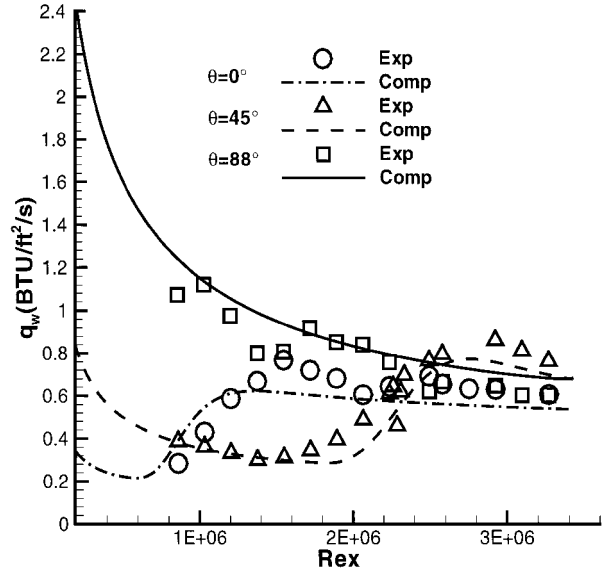

Fig. 5 Heat-flux distribution along the rays of cone (Re/L = 1.03 × 10^6/ft, HIDE).

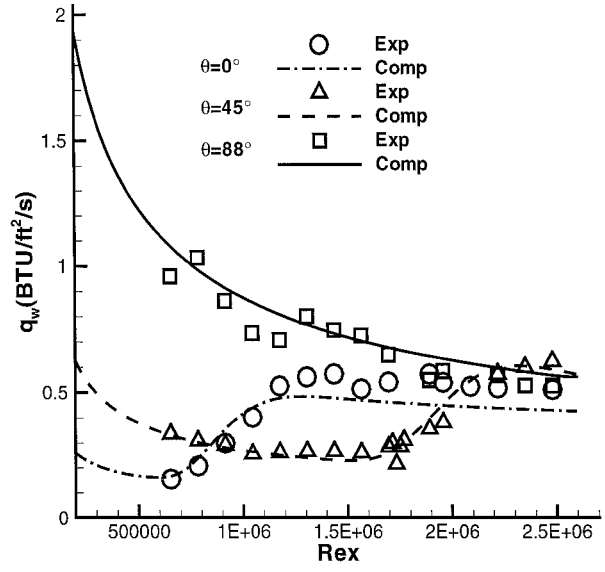

Fig. 6 Heat-flux distribution along the rays of cone (Re/L = 7.8 × 10^5/ft, HIDE).

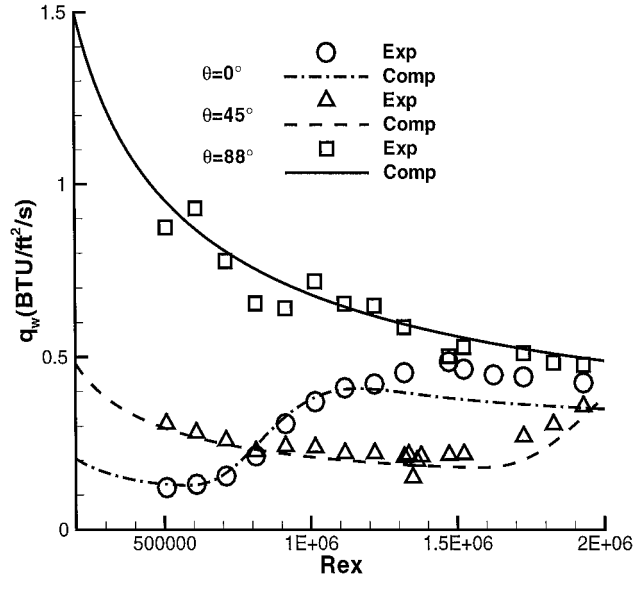

Fig. 7 Heat-flux distribution along the rays of cone (Re/L = 6.09 × 10^5/ft, HIDE).

at $Re/L = 1.98 \times 10^6$/ft. For the lower Reynolds numbers transition does not extend to the leading edge.

As is seen from Fig. 2, τ_{bp} is much larger than either τ_{sm} or τ_{cf}. Because of this, coupling the HIDE mode with the other modes does not change much the results shown in Figs. 4–7. Thus, it is concluded that the HIDE mode is the mode that better reproduces experimental results.

Although the present theory seems to suggest that a bypass mechanism resulting from the high turbulent intensity in the tunnel is responsible for observed transition, we cannot rule out that this mechanism can also be a result of interactions in the nonlinear regions. These nonlinear interactions can involve dominant instability mechanisms in the linear regions such as second mode, crossflow, and possibly others yet to be determined. The important point that Mokovin[1] tried to make is that the so-called bypass transition, of which HIDE is a subset, cannot be described by linear stability theory. Because of this, it appears to be inappropriate to assume that all transition mechanisms are a result of first, second, stationary, and traveling crossflow modes. Some of these modes exist in the flow, but evidently they are not the ones directly responsible for transition. The fact that Poggie et al.[4] were unable to identify the dominant instability mechanism in the flow suggests the existence of other mechanisms and points the need for additional experiments in quiet tunnels using the configuration considered here.

Conclusions

The present work represents the first successful attempt at calculating three-dimensional transitional flows in conventional hypersonic facilities. Moreover, it suggests that the dominant transition mechanism is a form of a bypass mechanism resulting from large-amplitude disturbances. Although the high freestream fluctuation intensity is a major contributing factor to the instability mechanism, we cannot rule out at this time the influence of the nonlinear interactions involving instability waves that are prominent in the linear growth region. It is going to take additional experiments and additional computations of three-dimensional configurations before a definitive understanding of three-dimensional transitional flow emerges.

Acknowledgments

Xudong Xiao acknowledges the support of North Carolina State University. J. R. Edwards and H. A. Hassan acknowledge the partial support of Sandia National Laboratories under Grant BF-0856. The authors acknowledge many helpful discussions with Ndaona Chokani. In addition, they express their appreciation to Roger Kimmel for providing the experimental data. Computer resources were provided by the North Carolina Supercomputing Center.

References

[1]Mokovin, M. V., "Bypass Transition to Turbulence and Research Desiderata," *Transition in Turbines*, edited by R. W. Graham, NASA CP 2386, 1985, pp. 161–204.

[2]Roshetko, E., "Transient Growth: A Factor in Bypass Transition," *Physics of Fluids*, Vol. 13, No. 5, 2001, pp. 1067–1075.

[3]Kimmel, R. L., Poggie, J., and Schwoerke, S. N., "Laminar-Turbulent Transition in a Mach 8 Elliptic Cone Flow," *AIAA Journal*, Vol. 37, No. 9, 1999, pp. 1080–1087.

[4]Poggie, J., Kimmel, R. L., and Schwoerke, S. N., "Traveling Instablity Waves in a Mach 8 Flow over an Elliptic Cone," *AIAA Journal*, Vol. 38, No. 2, 2000, pp. 251–258.

[5]Donaldson, J., and Coulter, S., "A Review of Free-Stream Flow Fluctuation and Steady-State Flow Quality Measurements in the AEDC/VKF Supersonic Tunnel A and Hypersonic Tunnel B," AIAA Paper 95-6237, April 1995.

[6]Warren, E. S., and Hassan, H. A., "Transition Closure Model for Predicting Transition Onset," *Journal of Aircraft*, Vol. 35, No. 5, 1998, pp. 769–775.

[7]McDaniel, R. D., and Hassan, H. A., "Study of Bypass Transition Using the k–ζ Framework," AIAA Paper 2000-2310, June 2000.

[8]McDaniel, R. D., Nance, R. P., and Hassan, H. A., " Transition Onset Prediction for High Speed Flow," *Journal of Spacecraft and Rockets*, Vol. 37, No. 3, 2000, pp. 304–309.

[9]McDaniel, R. D., and Hassan, H. A., "Transition Mechanisms in Conventional Hypersonic Facilities," *Journal of Spacecraft and Rockets*, Vol. 38, No. 2, 2001, pp. 180–184.

[10]Warren, E. S., and Hassan, H. A., "A Transition Model for Swept Wing Flows," AIAA Paper 97-2245, June 1997.

[11]Robinson, D. F., and Hassan, H. A., "Further Development of the k–ζ (Enstrophy) Turbulence Closure Model," *AIAA Journal*, Vol. 36, No. 10, 1998, pp. 1825–1833.

[12]Müller, B., and Bippes, H., "Experimental Study of Instability Modes in a Three-Dimensional Boundary Layer," AGARD Rept. 438, Oct. 1988, pp. 13.01–13.15.

[13]Poggie, J., and Kimmel, R. L., "Travelling Instabilities in Elliptic Cone Boundary Layer Transition at Mach 8," AIAA Paper 98-0435, Jan. 1998.

[14]Wilcox, D. C., *Turbulence Modeling for CFD*, 2nd, ed., DCW Industries, Inc., La Cañada, CA, 1998, p. 204.

[15]Dhawan, S., and Narasimha, R., "Some Properties of Boundary Layer Flow During Transition from Laminar to Turbulent Motion," *Journal of Fluid Dynamics*, Vol. 3, No. 4, 1958, pp. 418– 436.

[16]Edwards, J. R., "A Low-Diffusion Flux-Splitting Scheme for Navier-Stokes Calculations," *Computer and Fluids*, Vol. 26, No. 6, 1997, pp. 635–659.

[17]Edwards, J. R., "Advanced Implicit Methods for Finite-Rate Hydrogen-Air Combustion Calculations," AIAA Paper 96-3129, July 1996.

[18]Saad, Y., and Shultz, M. H., "GMRES: A Generalized Minimum Residual Algorithm for Solving Nonsymmetric Linear System," *SIAM Journal of Scientific and Statistical Computation*, Vol. 7, No. 3, 1986, p. 856.

T. C. Lin
Associate Editor